
MAXIMUM SCOUR DEPTH AT SUBMERGED SKEWED BRIDGE AND PIER

Amirsaeed Farhangi*, Ahmad Mohammad Ali Thamer, Abdul Halim Ghazali & Badronnisa Yusuf

Department of Civil Engineering, University Putra Malaysia, 43400 UPM Serdang, Selangor Darul Ehsan, Malaysia

*Corresponding Author: asfarhangi@yahoo.com

Abstract: Maximum local scour depth around pier due to the submerged skewed bridge along with its rectangular pier under clear water condition has been experimentally studied. In present study, twenty four tests were carried out including; six various aligned bridge models with the different angles such as; 0, 5, 10, 15, 22.5 and 30 degree to the presumptive perpendicular line to the flume wall under two flow types of fully and partially submerged bridge above two different median sizes of uniform sediments. However, in the present study, aligned factor in pressure flow is experimentally evaluated, its results are much less than aligned factor in free flow in the same ratio of rectangular pier length to the pier width. Also, the relationship between dependent and independent variables firstly was determined. Thereafter, an equation was acceptably proposed by using dimensional analysis, collected data and multiple linear regressions.

Keywords: *Bridge pier, bridge thickness, maximum scours depth, submerged bridge*

1.0 Introduction

Bridges failures across rivers and their prospective affliction not only caused loosing life and cars, but also brought huge expenditure for bridge repair or reconstruction to the governments. Existence of hydraulic structures as an obstacle in the face of flow creates a phenomenon which has enough potential to remove bed grains around as local scour (Pal *et al.*, 2012; Sarkar *et al.*, 2015). As Briaud *et al.* (2014) cited that scour has played the most destructive role in bridge failure in the United State. To evaluate mentioned problem, researchers have already studied about it for several decades. They found that pier as an obstacle convert normal stream flow to the downward flow, horseshoe vortices and wake vortices that cause dislodging of bed grains around the pier. This phenomenon that attributed to local scour depth around pier potentially depends to the characteristics of approach flow, pier, sediment and time (Melville, 2000). In this subject, many researchers tried to evaluate and predict scour depth around bridge foundation. Although they widely analyzed various conditions, most of them studied

about it under free flow. But some limitations around the river do not allow for constructing high level bridges to avoid submergence during high floods (Verma *et al.*, 2004). As Shen *et al.* (2012) stated that a large number of bridges in the U.S.A. have the potential to be inundated. Recently, some researchers such as; Umbrell *et al.* (1998) and Guo *et al.* (2010) attempted to evaluate local scour under pressure flow (submerged bridge) but these studies still suffer from different flow alignment toward the bridge deck, especially along with its pier wherein changes of flow direction in high abnormal flood are probable. In present study, maximum scour depth around submerged bridge pier due to various alignments of bridge deck under clear water condition has been experimentally evaluated.

2.0 Materials and Methods

2.1 Flume and Bridge Models

Present experimental research carried out at the hydraulics and coastal laboratory in National Hydraulic Research Institute of Malaysia (NAHRIM), Kuala Lumpur, Malaysia. A large flume 51 m long, 1.5 m wide and 2 m deep with a recession almost at the middle with 9.5 m long, 1.5 m width and 0.50 m deep was utilized. There was a centrifugal pump with the maximum discharge capacity of $0.135 \text{ m}^3/\text{s}$ at the end of flume and flow could be circulated back through a pipe toward the flume head. The pump could be fixed on required discharge during each run. Flow depth could be also fixed before switching on the pump with two inlet (pouring) and an outlet (draining) pipes wherein an inlet pipe were installed at the beginning of the flume and another one along with outlet one were arranged at the end of flume respectively (Figure 1).

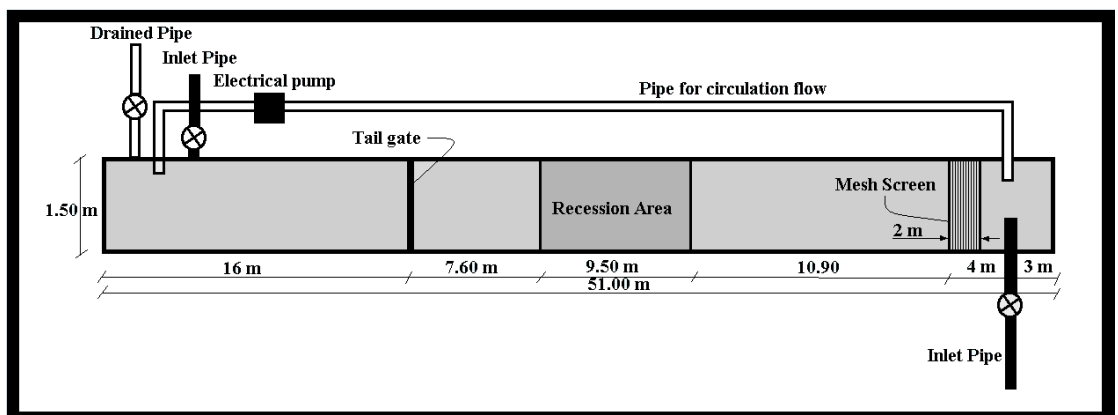


Figure 1: Schematic plan of NAHRIM flume.

A point gauge with the accuracy of $\pm 0.1\text{mm}$ could cover an area ($1.5\text{m} \times 4.74\text{m}$) above the recession site to survey bed level changes around the submerged bridge model due to the flume width and carriage wagon movement on the rail respectively. There was also a portable flow meter to measure the flow velocity in various flow depths. Six different steel aligned bridge models along with a pier were constructed in several pieces including frame with two square girders which were longitudinally welded under the frame, some plates could cover the frame area as bridge deck and a rectangular pier 40 cm long and 4 cm wide in the ratio of $l/b = 40/4 = 10$. Rectangular pier could be perpendicularly installed under each aligned bridge deck (Figure 2).

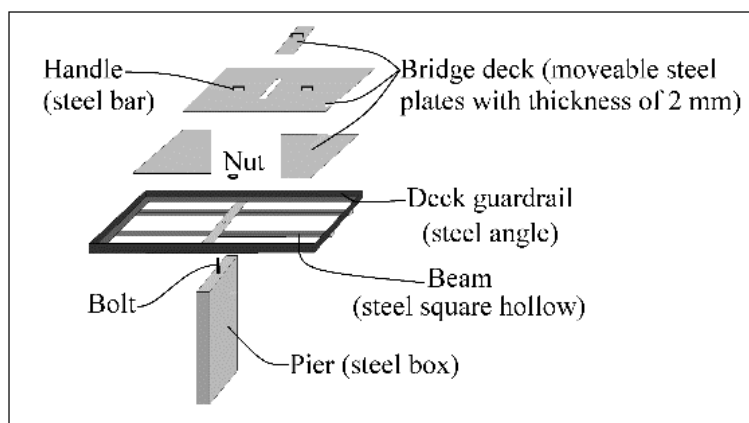


Figure 2: Schematically pieces of model.

The ratio of pier width to the flume width is $4/150 = 0.03$ or 3% where Chiew and Melville (1987) defined that pier nose width limitation should be less than 10% of flume width to avoid the flume wall effect on scour hole around pier as Masjedi *et al.* (2010) cited. Each bridge deck could be fixed and tighten above the pier by nuts and bolts and could stand in different alignments of 0, 5, 10, 15, 22.5 and 30 degree (Figure 3). Each model was tested in two various flow types of partially and fully submerged bridge and two different uniform sediment sizes. The ratio of pier wide to the both sediments mean sizes of 0.23 mm and 0.80 mm are 174 and 50 respectively where it should be $b/d_{50} \geq 50$ to prevent the effect of the bed grain size on scour depth (Zarrati *et al.*, 2010). The geometric standard deviations of above sediment sizes are also 1.29 and 1.31 respectively. As Ettema *et al.* (1998a) expressed that sediment sizes in laboratory experiment for scour around pier according to the most sandy river sites should be considered which is in average particle sizes of about 0.1 to 10 mm .

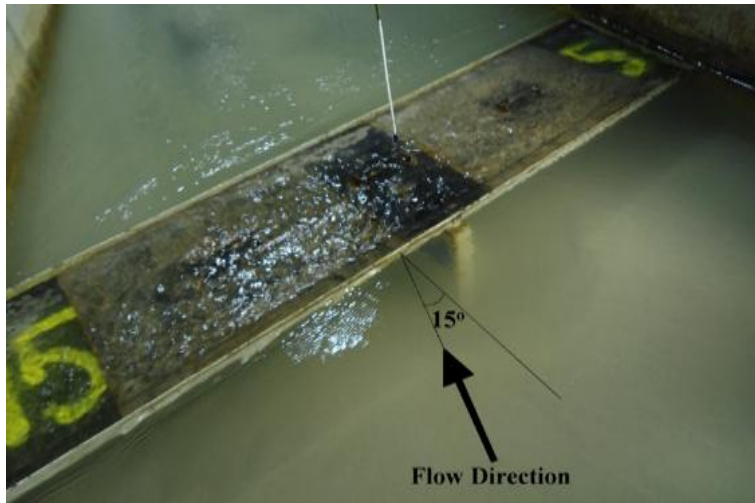


Figure 3: Fully submerged bridge model in the alignment of 15°.

2.2 Method

At the beginning of each run, proposed bridge model was installed above the recession site and sediment were smoothly leveled before opening valves of inlet pipes from both sides of flume and pouring water up to the proper level either higher than high chord of bridge deck or lower than it at the bridge deck thickness as fully or partially submerged bridge respectively. After fixing water level, pump was switched on and gradually increased discharge which directly increased flow velocity in the same flow depth. In this step, it was tried to adjust flow velocity from 0.7 to 0.8 of critical velocity by measuring flow velocity. In fact, for having clear water condition, approach flow velocity had to be considered less than threshold velocity (critical velocity). In this subject, Arneson (1977) evaluated incipient motion due to bed grain size in following equation as it is cited by (Lyn, 2008).

$$V_c = 1.52 \sqrt{g(s_g - 1)d_{50}} \left(\frac{y_u}{d_{50}} \right)^{(1/6)} \quad (1)$$

where g = acceleration of gravity, s_g = sediment specific gravity, y_u = approach flow depth and d_{50} = median sediment diameters.

Maximum scour depths at the pier nose was measured in proper unequal periods including; 0, 10, 20, 30, 40, 50, 60, 75, 90, 105, 120, 150, 180, 210, 240 minutes thereafter hourly up to the end of run. Each run ended while two interval measurements of maximum scour depths were almost equal (about 9 to 12 hours). After switching off

the pump, valve of outlet pipe was opened to gradually drain flume water without any transporting sediment and finally, surveying of bed level around pier and bridge deck as 3-D measurement were carried out (Figure 4).

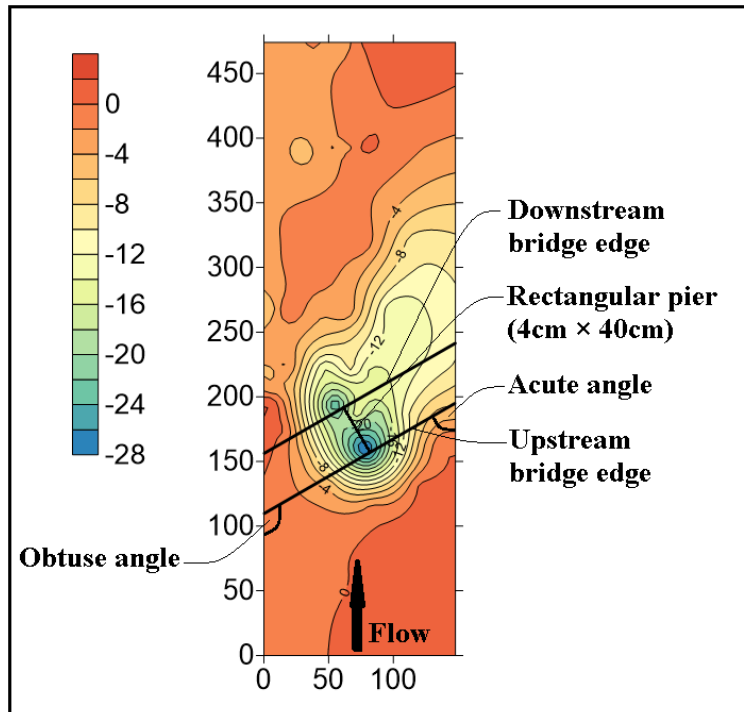


Figure 4: Surveying map at the end of run under model of 8030PP¹.

2.3 Extension of Maximum Scour Depth to the Equilibrium Scour Depth

All measured of maximum scour depths at the end of each run converted to the equilibrium scour depths. In this subject, all measured scour depth extended to equilibrium scour depth as Melville and Chiew (1999) estimated it as following equation:

¹Each model code shows run condition with four numbers and two letters. First and second two numbers are attributed to median sediment size and flow alignment in degree respectively. First letter shows flow types of fully or partially submerged bridge and last letter shows the pier existence. For instance, 2315FP shows that this run was under following condition; (median sediment size = 0.23 mm, flow alignment = 15° and fully submerged bridge in presence of pier).

$$\frac{ds}{ds_e} = \exp \left\{ -0.03 \left| \frac{V_c}{V_u} \cdot \ln \left(\frac{t}{t_e} \right) \right|^{1.6} \right\} \quad (2)$$

where d_{se} = equilibrium scour depth, d_s = scour depth, V_u = approach velocity, V_c = critical velocity, t = time related to scour depth of ds and t_e = ultimate time related to equilibrium scour depth that can be estimated by following equations:

$$t_e(\text{days}) = 48.26 \frac{B}{V_u} \left(\frac{V_u}{V_c} - 0.4 \right) \quad \text{if} \quad \frac{y_u}{B} > 6, \quad \frac{V_u}{V_c} > 0.4 \quad (3)$$

$$t_e(\text{days}) = 30.89 \frac{B}{V_u} \left(\frac{V_u}{V_c} - 0.4 \right) \left(\frac{y_u}{B} \right)^{0.25} \quad \text{if} \quad \frac{y_u}{B} \leq 6, \quad \frac{V_u}{V_c} > 0.4 \quad (4)$$

where B = pier width and y_u = approach flow depth.

It should be mentioned that all measured maximum scour depths at the end of each run modified to the equilibrium scour depths and used for all calculation.

3.0 Results and Discussion

3.1 Effective Factors on Scour Depth at Submerged Bridge

Melville and Coleman (2000) expressed that the effective factors on scour depth around pier under free flow can be categorized as following:

$$y_s = f \left[\text{Flood flow } (\rho, \nu, V_u, y_u, g, P_1), \text{ Bed sediment } (d_{50}, \sigma_g, \rho_s, V_c), \text{ pier geometry } (B, S, K_\theta), \text{ Time } (t) \right] \quad (5)$$

where y_s = scour depth; ρ and ν = fluid density and kinematic viscosity respectively; V_u and y_u = approach flow velocity and flow depth respectively; g = acceleration of gravity; P_1 = the upstream flow static pressure; d_{50} and σ_g = median size and geometric standard deviation of the bed grain size distribution respectively; ρ_s = sediment density; V_c = critical velocity due to bed grains; B = pier width; S = pier shape; K_θ = correction factor for pier alignment; and t = time.

Moreover, some other factors related to bridge geometry under submergence should be added to Equation (5) as following:

Effective bridge thickness (a): including girders and guard rails thickness in touch with flow as a horizontal obstacle which creates vertical contraction to the flow stream (Figure 5).

$$a = \min (h_u - h_b, b) \quad (6)$$

where b = real bridge deck thickness.

Bridge opening depth (h_b): it influences on initial cross sectional area and flow velocity under pressure flow.

Flow head over the bridge deck (w): although it does not pass through bridge opening, creates trilling vortices above bridge deck.

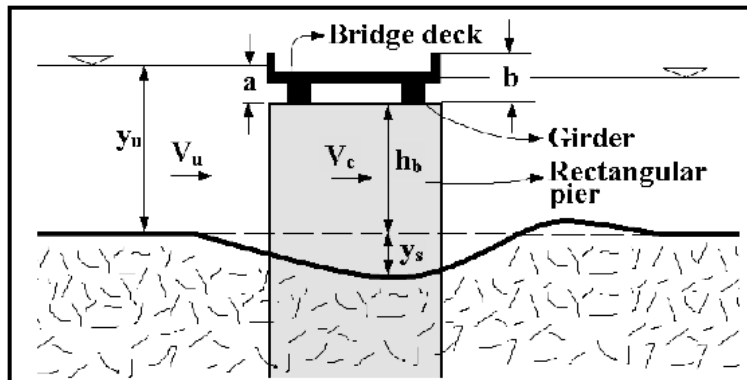


Figure 5: Longitudinal profile of flume.

Therefore, new category under pressure flow can be added as:

$$y_s = f [\text{Flood flow } (\rho, v, V_u, y_u, g, P_1), \text{ Bed sediment } (d_{50}, \sigma_g, \rho_s, V_c), \text{ pier Geometry } (B, S, K_\theta), \text{ Time } (t), \text{ Bridge geometry in pressure flow } (a, h_b, w)] \quad (7)$$

Equation (7) can be rewritten as following:

$$y_s = f [\rho, v, V_u, y_u, g, P_1, d_{50}, \sigma_g, \rho_s, V_c, B, S, K_\theta, t, a, h_b, w] \quad (8)$$

Some independent variables can be neglected such as; upstream flow static pressure that depends on flow depth, flow viscosity, flow density and sediment density. Therefore, Equation (8) can be simplified to:

$$y_s = f [V_u, y_u, g, d_{50}, \sigma_g, V_c, B, S, K_\theta, t, a, h_b, w] \quad (9)$$

Dimensional analysis under submerged bridge leads to the dimensionless function relation as following:

$$\frac{y_s}{h_b} = f \left(\frac{V_u}{V_c}, \frac{B}{d_{50}}, \frac{a}{y_u}, \frac{w}{y_u}, \frac{B}{y_u}, S, K_\theta, \sigma_g, \frac{V_u t}{B}, \frac{V_u}{\sqrt{g y_u}}, \frac{y_u}{d_{50}} \right) \quad (10)$$

In present study, some terms in Equation (10) can be removed such as; repeated and fixed factors and geometric standard deviation because of uniform sediment size that directly depends to the critical velocity as following:

$$\frac{y_s}{h_b} = f \left(\frac{V_u}{V_c}, \frac{B}{y_u}, \frac{a}{y_u}, K_\theta \right) \quad (11)$$

Among all above independent factors, aligned factor (K_θ) has the most effectiveness on scour depth. As Melville (2008) expressed that align factor (K_θ) strongly effects on local scour depth around all pier shape excluding circular one and by increasing pier alignment, scour depth strongly increases too.

Correction factor for pier alignment (K_θ) in free flow has been evaluated by Ettema *et al.* (1998b) as following:

$$K_\theta = \left(\frac{l}{B} \sin \theta + \cos \theta \right)^{0.65} \quad (12)$$

where l = rectangular pier long and B = rectangular pier width.

But in present study ($l/B = 10$), aligned factor in pressure flow (K_θ) experimentally evaluated by dividing each equilibrium scour depth of aligned bridge deck along with its pier to the equilibrium scour depth of non-aligned one ($\theta = 0$) where they are much less than aligned factor in free flow in the same ratio of $l/B = 10$ (Figure 6).

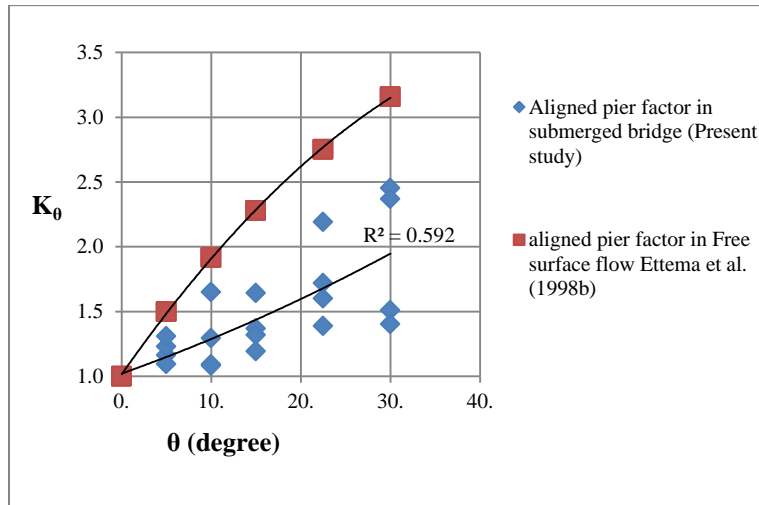


Figure 6: Comparison of aligned factor between free surface flow and pressure flow.

Following equation can be utilized to calculate the aligned factor (K_θ) in submerged bridge:

$$K_\theta = 1 + 0.0001\theta^2 + 0.0272\theta \quad \text{where} \quad 0^\circ \leq \theta \leq 30^\circ \quad (13)$$

Reduction of aligned factor in submerged bridge in comparison to free surface flow may occur by deflecting some part of approaching flow depth at the skewed bridge deck thickness. It could be obviously observed during experiments by transferring floating material at the aligned bridge thickness toward flume wall where the connection between bridge deck and flume wall makes an acute angle.

3.2 Maximum Scour Depth around Pier

Twenty four tests of submerged bridge with pier have been done in six different alignments with two flow types of fully and partially submerged bridge on two different uniform median sizes of sediment under clear water (Table 1).

Table 1: Collected laboratory data under submerged bridge pier.

Row	Model	θ	d_{50}	Time	V_u	V_c	h_b	y_u	a	Y_s
		(-)	(mm)	(hr)	(m/s)	(m/s)	(m)	(m)	(m)	measurement
1	8000PP	0	0.80	9	0.40	0.46	0.14	0.19	0.06	0.115
2	8005PP	5	0.80	9	0.39	0.45	0.14	0.19	0.05	0.134
3	8010PP	10	0.80	9	0.41	0.45	0.14	0.19	0.05	0.191
4	8015PP	15	0.80	9	0.39	0.46	0.15	0.20	0.05	0.189
5	8022PP	22.5	0.80	9	0.41	0.46	0.15	0.21	0.06	0.253
6	8030PP	30	0.80	11	0.41	0.47	0.17	0.23	0.06	0.287
7	8000FP	0	0.80	9	0.39	0.46	0.13	0.22	0.06	0.126
8	8005FP	5	0.80	9	0.38	0.47	0.15	0.23	0.06	0.137
9	8010FP	10	0.80	9	0.39	0.47	0.15	0.23	0.06	0.162
10	8015FP	15	0.80	9	0.42	0.47	0.15	0.23	0.06	0.173
11	8022FP	22.5	0.80	9	0.40	0.47	0.16	0.24	0.06	0.216
12	8030FP	30	0.80	11	0.42	0.46	0.14	0.22	0.06	0.304
13	2300PP	0	0.23	11	0.24	0.31	0.21	0.26	0.04	0.092
14	2305PP	5	0.23	11	0.24	0.31	0.21	0.25	0.04	0.114
15	2310PP	10	0.23	11	0.23	0.31	0.22	0.26	0.05	0.101
16	2315PP	15	0.23	11	0.24	0.31	0.22	0.26	0.05	0.110
17	2322PP	22.5	0.23	12	0.24	0.32	0.24	0.28	0.04	0.130
18	2330PP	30	0.23	12	0.23	0.32	0.25	0.28	0.04	0.141
19	2300FP	0	0.23	11	0.23	0.32	0.23	0.31	0.06	0.086
20	2305FP	5	0.23	11	0.23	0.32	0.21	0.29	0.06	0.113
21	2310FP	10	0.23	11	0.23	0.32	0.21	0.29	0.06	0.093
22	2315FP	15	0.23	12	0.23	0.32	0.22	0.31	0.06	0.115
23	2322FP	23	0.23	12	0.23	0.32	0.22	0.31	0.06	0.140
24	2330FP	30.0	0.23	12	0.23	0.32	0.24	0.33	0.06	0.123

Present study tried to produce an equation to predict the maximum scour depth around pier in submerged bridge under clear water by using all relationship between independent and dependent variables due to Equation (11). Multiple linear regressions (MLR) are statistical technique model that can evaluate the best relationship between two or more variables by a linear equation as following:

$$Y = C_0 + C_1X_1 + C_2X_2 + C_3X_3 + \dots + C_nX_n \tag{14}$$

where Y is function of different variables including $X_1, X_2, X_3, \dots, X_n$ and $C_0, C_1, C_2, C_3, \dots, C_n$ are constant and coefficients.

This model was used to predict the maximum scour depth according the dimensional analysis. For checking result of maximum scour depth prediction, sixteen data of twenty four experiments (2/3 of all collected data) randomly selected to be utilized in multiple linear regressions.

To randomly choose and keep the eight remain series of data for final checking, number seven was chosen to be periodically counted and selected them. Therefore, every other seven data were selected (each selected series of data were omitted from repeated counting). Selected series are; 7, 14, 21, 4, 12, 20, 5 and 15. These series of data can be acceptably chosen because they are including of four selection in each partially or fully submerged flow; four selections of both sediment sizes and having all various alignments (Table 2).

The remains 16 series of data were used in multiple linear regressions (MLR). Thus, $y_s/(h_b \cdot K_\theta)$ as dependent and V_u/V_c , a/y_u and B/y_u as three independent variables can be substitute to Y , X_1 , X_2 and X_3 respectively. In this subject, all coefficients are attained as $C_1 = +1.74819$, $C_2 = +2.63834$, $C_3 = +1.52073$ and $C_o = -1.55321$. So, suggested equation to predict maximum scour depth around pier can be written as following:

$$\frac{y_s}{h_b} = \left[1.74819 \left(\frac{V_u}{V_c} \right) + 2.63834 \left(\frac{a}{y_u} \right) + 1.52073 \left(\frac{B}{y_u} \right) - 1.55321 \right] \cdot K_\theta \quad (15)$$

The R^2 between equilibrium and predicted scour depth due to equation (15) is 0.9119 (Figure 7).

Table 2: All and sixteen selected data series in using multiple linear regressions (MLR) method.

Row	Model	K_θ	$d_s/(h_b \cdot K_\theta)$	V_u/V_c	a/γ_u	B/γ_u	γ_s Equilibrium	γ_s prediction	Abs. Error
		(-)	(-)	(-)	(-)	(-)	(m)	(m)	(m)
1	8000PP	1.00	0.92	0.88	0.30	0.21	0.126	0.148	0.021
2	8005PP	1.14	0.93	0.86	0.26	0.22	0.147	0.151	0.004
3	8010PP	1.28	1.17	0.90	0.27	0.21	0.208	0.188	0.021
4*	8015PP	1.43	0.99	0.85	0.27	0.20	0.207	0.199	0.008
5*	8022PP	1.66	1.12	0.89	0.29	0.19	0.277	0.260	0.017
6	8030PP	1.91	0.95	0.87	0.26	0.17	0.310	0.301	0.008
7*	8000FP	1.00	1.03	0.84	0.28	0.18	0.138	0.124	0.014
8	8005FP	1.14	0.91	0.81	0.26	0.18	0.151	0.139	0.012
9	8010FP	1.28	0.92	0.83	0.26	0.17	0.179	0.162	0.016
10	8015FP	1.43	0.88	0.90	0.26	0.17	0.189	0.208	0.018
11	8022FP	1.66	0.89	0.85	0.25	0.17	0.238	0.224	0.014
12*	8030FP	1.91	1.24	0.90	0.27	0.18	0.327	0.272	0.055
13	2300PP	1.00	0.49	0.77	0.17	0.16	0.105	0.102	0.002
14*	2305PP	1.14	0.55	0.78	0.17	0.16	0.129	0.115	0.014
15*	2310PP	1.28	0.41	0.74	0.17	0.15	0.114	0.118	0.004
16	2315PP	1.43	0.40	0.77	0.18	0.15	0.125	0.150	0.026
17	2322PP	1.66	0.37	0.76	0.15	0.14	0.145	0.156	0.011
18	2330PP	1.91	0.34	0.73	0.14	0.14	0.158	0.137	0.021
19	2300FP	1.00	0.42	0.72	0.19	0.13	0.098	0.094	0.004
20*	2305FP	1.14	0.53	0.72	0.21	0.14	0.128	0.113	0.015
21*	2310FP	1.28	0.39	0.72	0.20	0.14	0.106	0.125	0.019
22	2315FP	1.43	0.42	0.72	0.20	0.13	0.129	0.128	0.001
23	2322FP	1.66	0.43	0.72	0.20	0.13	0.157	0.152	0.004
24	2330FP	1.91	0.31	0.71	0.18	0.12	0.138	0.163	0.026

Symbol (*) indicates eight random selected models for final checking the suggested equation.

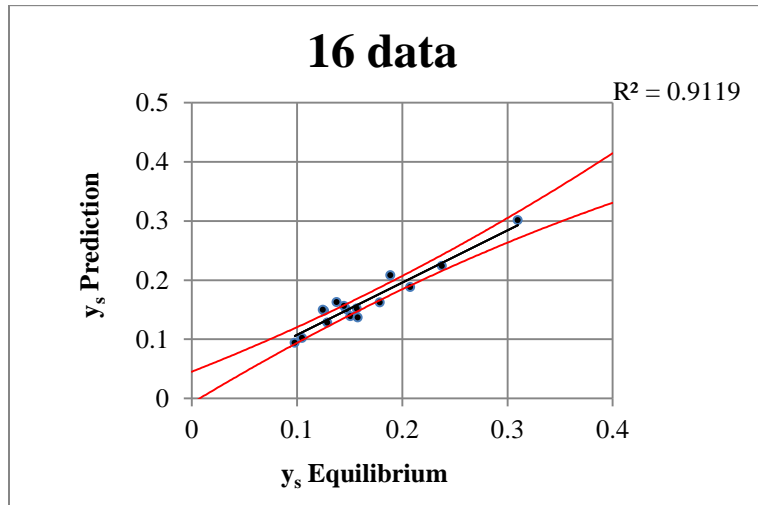


Figure 7: Comparison the maximum scour depth prediction versus measured by 95% confidence level.

Now, the eight selected series data that were not associated in equation (15) should be evaluated for checking the ability of suggested equation. Comparison between predicted and equilibrium scour depth shows proper $R^2=0.9634$ (Figure 8).

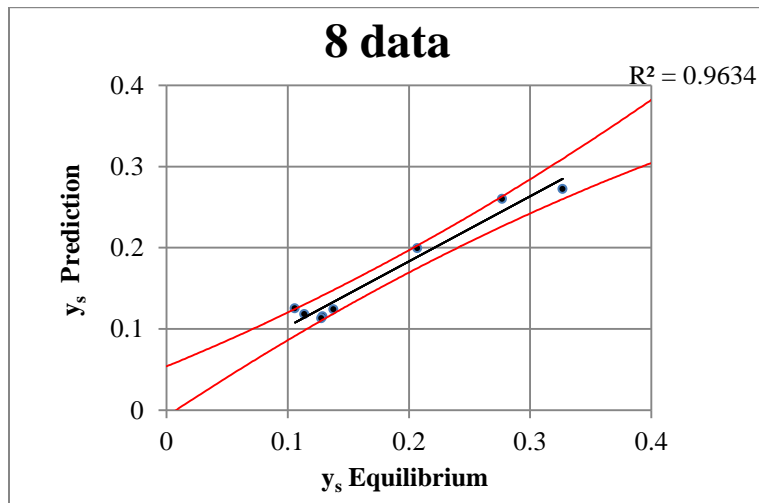


Figure 8: Comparison the maximum scour depth prediction versus measured in selected data series by 95% confidence level.

According to Table (2) and using mean root square of all twenty four series of data is 0.018 m and shows $R^2 = 0.926$ (Figure 9).

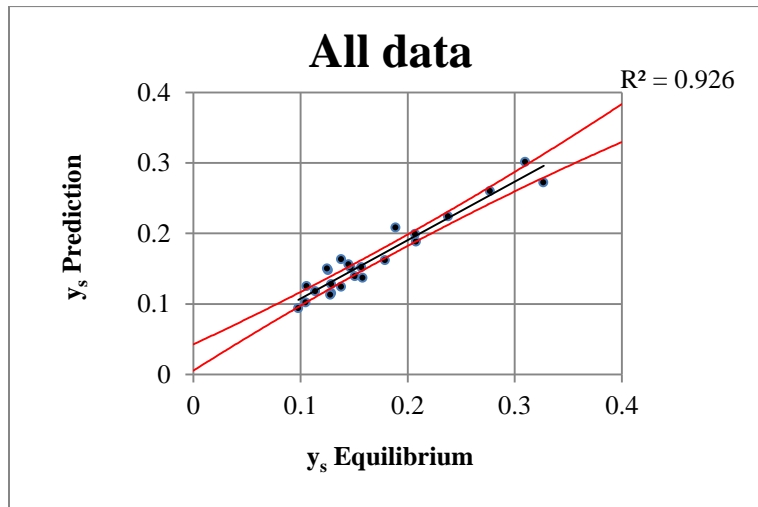


Figure 9: Comparison of all prediction versus measured data by 95% confidence level.

4.0 Conclusion

Maximum scour depth around rectangular pier under submerged aligned bridge and clear water condition can be predicted by Equation (15). Also, Approach flow direction after impinging to the aligned bridge thickness tends to move toward the acute angle of flume wall and upstream bridge deck connection and it increases by increasing the angle between approach flow and presumptive perpendicular line to the bridge deck. Therefore, focused flow direction at the bridge deck toward acute angle makes deeper scour wall after downstream edge of bridge and also accumulates sediment heap in higher level than opposite side (obtuse angle).

5.0 Acknowledgements

The authors would like to express special thanks to Mr. Haji Fauzi and his entire colleague at the hydraulic & instrumentation laboratory in NAHRIM for all assistance.

References

- Arneson, L.A. (1997), "The effect of pressure-flow on local scour in bridge opening," Ph.D. thesis, Dept. of Civil Engineering, Colorado State University, Fort Collins, CO.
- Briaud, J. L., Gardoni, P., and Yao, C., (2014). *Statistical, Risk, and Reliability Analyses of Bridge Scour*. Journal of Geotechnical and Geoenvironmental Engineering, 140: 1-10
- Ettema, R., Melville, B. W., and Barkdole, B., (1998a). *Scale Effect in Pier- Scour Experiments*. Journal of Hydraulic Engineering, 124: 639-642.
- Ettema, R., Mostafa, E. A., Melville, B. W., and Yassin, A. A., (1998b). *Local Scour at Skewed Piers*. Journal of Hydraulic Engineering, 124: 756-759.
- Guo, J., Kerényi, K., Pagan-Ortiz, J.E., Flora, K., and Afzal, B., (2010). *Submerged- Flow Bridge Scour under Maximum Clear- Water Condition (I)*. San Francisco, 5th international conference on scour and erosion, 807-814.
- Lyn, D. A., (2008). *Pressure-Flow Scour: A Reexamination of the HEC-18 Equation*. Journal of Hydraulic Engineering, 134: 1015- 1020.
- Masjedi, A., Shafaei Bejestan, M. and Esfandi, A., (2010). *Reduction of local scour at a bridge pier fitted with a collar in a 180 degree flume bend (Case study: oblong pier)*. journal of Hydrodynamics, 22: 669–673.
- Melville, B., (2008). *The Physics of Local Scour at Bridge Piers*. Tokyo, Fourth International Conference on Scour and Erosion, 28-40
- Melville, B. W. and Chiew, Y.M., (1999). *Time scale for local scour at bridge piers*. Journal of Hydraulic Engineering, 125: 59- 65.
- Melville, B. W. and Coleman, S. E., (2000) *Bridge Scour*. Auckland: Water Resources Publication, LLC., 192 pp.
- Pal, M., Singh, N. K. and Tiwari, N. K., (2012). *M5 Model Tree for Pier Scour Prediction Using Field Dataset*. Journal of Civil Engineering, 16: 1079-1084.
- Sarkar, K., Chakraborty, C. and Mazumder, B. S., (2015). *Spacetime dynamics of bed forms due to turbulence around submerged bridge piers*. Stoch Environ Res Risk Assess, 29: 995-1017.
- Shen, J., Shan, H., Suaznabar, O., Suaznabar, O., Zhaoding, X., Bojanowski, C., Lottes, S., and Kerényi, K., (2012). *Submerged-flow bridge scour under clear-water conditions*. ICSE6 Paris, 755-760.
- Umbrell, E. R., Kenneth Young, G., Stein, S. M. and Sterling Jones, J., (1998). *Clear-water contraction scour under bridges in pressure flow*. Journal of Hydraulic Engineering, 124: 236- 240.
- Verma, D. S., Setia, B. and Bhatia, U., (2004). *Constriction scour in pressurized flow condition*. International Journal of Engineering-Transactions, 17: 237-246.
- Zarrati, A. R., Chamani, M. R., Shafaie, A. and Latifi, M., (2010). *Scour countermeasures for cylindrical piers using riprap and combination of collar and riprap*. Sediment Research, 25: 313-321.